

GEOLOGICAL
CIRCULAR
78-2



Regional Distribution of Fractures in the Southern Edwards Plateau and Their Relationship to Tectonics and Caves

By
E. G. Wermund, Joseph C. Cepeda, and P. E. Luttrell



Bureau of Economic Geology
The University of Texas at Austin

W. L. Fisher, Director

1978



GEOLOGICAL
CIRCULAR
78-2

Regional Distribution of Fractures in the Southern Edwards Plateau and Their Relationship to Tectonics and Caves

By
E. G. Wermund, Joseph C. Cepeda, and P. E. Luttrell



Bureau of Economic Geology
The University of Texas at Austin

W. L. Fisher, Director

1978



Contents

ABSTRACT	1
INTRODUCTION	1
GENERAL GEOLOGY	2
METHODOLOGY FOR MAPPING FRACTURE ZONES	3
Fracture Trace Mapping	3
Digitization	3
Computation	3
Field Test	4
Caves	6
REGIONAL DISTRIBUTION OF FRACTURE ZONES AND CAVES	6
Short-Fracture Orientation	6
Short-Fracture Incidence	7
Long Fractures	9
Caves	9
METHODOLOGICAL BIAS	10
RELATION OF FRACTURES TO REGIONAL PHENOMENA	11
Fractures and Terrain	11
Fractures and Geology	11
Caves	12
MAJOR CONCLUSIONS	13
ACKNOWLEDGMENTS	13
REFERENCES	14
APPENDIX	14

FIGURES

1. Location of the southern Edwards Plateau in Texas	1
2. Geologic map of southern Edwards Plateau	2
3. A part of a controlled mosaic of black-and-white aerial photography	4
4. Areas of 36 quadrangles	5
5. Locations where field measurements of joints were determined in the test area	6
6. Orientation of joints in the test area displayed as rose diagrams with 10° classes	7
7. Orientation of fracture zones in the test area displayed as rose diagrams with 10° classes	8
8. End members of variable cave geometry shown as (A) oblate caves, and (B) linear caves	8
9. Orientation of short-fracture zones	9
10. Incidence of short-fracture zones	10
11. Long-fracture zones	11
12. Distribution and orientation of caves	12
13. Tectonic elements surrounding the southern Edwards Plateau	13

Regional Distribution of Fractures in the Southern Edwards Plateau and Their Relationship to Tectonics and Caves

By

E. G. Wermund, Joseph C. Cepeda, and P. E. Luttrell

ABSTRACT

In order to better understand the control exerted by fractures on the recharge and production zones of limestone aquifers, the authors delineated surficial fracture zones in the southern Edwards Plateau, Texas. Lineations were marked on nearly 200 mosaics the size of a standard 7.5-minute quadrangle with a scale of 1:24,000. Approximately 400 fracture zones were identified on each mosaic. Moving averages of the density and orientation of fracture zones were computed in order to map (1) number of fractures, (2) length of fracturing, (3) distribution of fracture intersections, (4) weighted arithmetic mean of fracture orientation in northeast and northwest quadrants, and (5) standard deviation of the means. All were calculated per unit area. In addition, rose diagrams were computed for selected areas, generally a standard 7.5-minute quadrangle.

The method introduced bias in that (1) fracture zones were identified with greater difficulty at the margins of mosaics, and (2) more north-south and east-west fracture zones were observed in field measurements than in aerial photographic interpretations.

The fractures appear controlled both by an old system of basement fracturing and by the trend of the relatively young Balcones fault system. The basement system contains prominent northeastward- and northwestward-trending sets, and north-south- and east-west-trending subsets. Fractures related to the Balcones fault zone trend east-west in the western Edwards Plateau and generally approach north in the eastern plateau. Cave passageways in the western plateau appear to parallel fracture zones trending

northwestward, northeastward, and westward, whereas abundant cave corridors of eastern caves commonly align with the principal faults of the Balcones fault zone.

INTRODUCTION

The anisotropic permeability of limestones is a major problem which complicates the management of carbonate aquifers. In many limestone aquifers it may be possible to study the vertical movement of fluids separately from their horizontal migration. A simplistic view suggests that the vertical porosity/permeability is controlled by fractures and faults, whereas variations in the horizontal porosity/permeability are dominated by facies differences both along bedding planes and in lateral transitions. In this study regional variations of fractures and faults are examined in order to better understand vertical control and, to a lesser degree, horizontal control of ground-water movement for a major limestone aquifer.

The study region (fig. 1) includes the Edwards Limestone aquifer, an especially valuable resource in south and southwest Texas. The aquifer is the sole source of potable water for the San Antonio metropolitan area, which has a population of over 773,248. The Edwards aquifer is also the only source of water for many other communities within 100 km of San Antonio, thereby supplying potable water to an additional half-million people. The aquifer also provides irrigation for approximately 2,600 km² of rich croplands.

The study region includes both the recharge and the producing zones for the Edwards Limestone

aquifer. The recharge zone is located in the southern part of a broad plateau, an area thoroughly dissected by headwardly sapping streams. Remnants of the plateau in the highest parts of the recharge zone remain at 730 m above sea level. Streams exit from the lowest part of the plateau at 230 m onto a broad, gently sloping plain which overlies the producing zone. Green (1967) summarized the work of earlier investigators and described the Edwards producing zone as approximately 200 km long and up to 50 km wide. In the zone, ground-water flow is confined between bounding faults and a downdip linear zone of increased salinity, the latter perhaps coinciding with a facies zone restricting circulation. The area

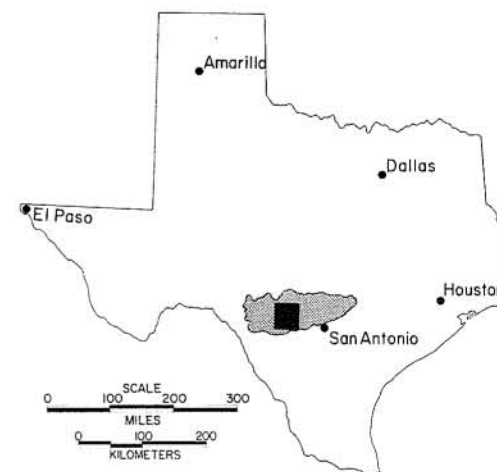


Figure 1. Location of the southern Edwards Plateau in Texas. Solid square west of San Antonio is a test area for experimental programs undertaken during the study.

studied in this report includes approximately 30,000 km², divided almost equally between zones of recharge and production.

Because the study region was large and research time was limited, it was not possible to determine vertical porosity by field measurements alone. A method was therefore developed of measuring fracture zones related to the identification of lineations on aerial photography, and then computer-processing that data. A description of this methodology and the correlation of results to the regional geology is the basis for the following study.

GENERAL GEOLOGY

A geological map (fig. 2) clearly defines the recharge and producing zones of the Edwards Limestone aquifer: the zones are separated by the southern limits of the Balcones fault zone (compiled from Barnes, project director, Geologic Atlas of Texas). North of the fault zone, the calcareous Glen Rose and Edwards formations dominate a dissected plateau. The regional dissection of the recharge zone in the northern part of the study area can be clearly differentiated into (1) a western quarter with most land in flat divides, (2) a west-central quarter with

most land in valley slopes, and (3) an eastern half with most land in valley floors. In the area of the measured reference section (fig. 2), the Glen Rose Formation is more than 145 m thick; the Edwards Limestone is about 120 m thick (Rose, 1972).

The Glen Rose Formation is composed of alternating beds of limestone, dolomite, and soft marly limestones which erode to recessive slopes. About 60 percent of the stratigraphic section is formed of these soft limestones. Conversely, the overlying Edwards formation is composed of limestone and dolomite, with only 8 percent soft marly limestone in

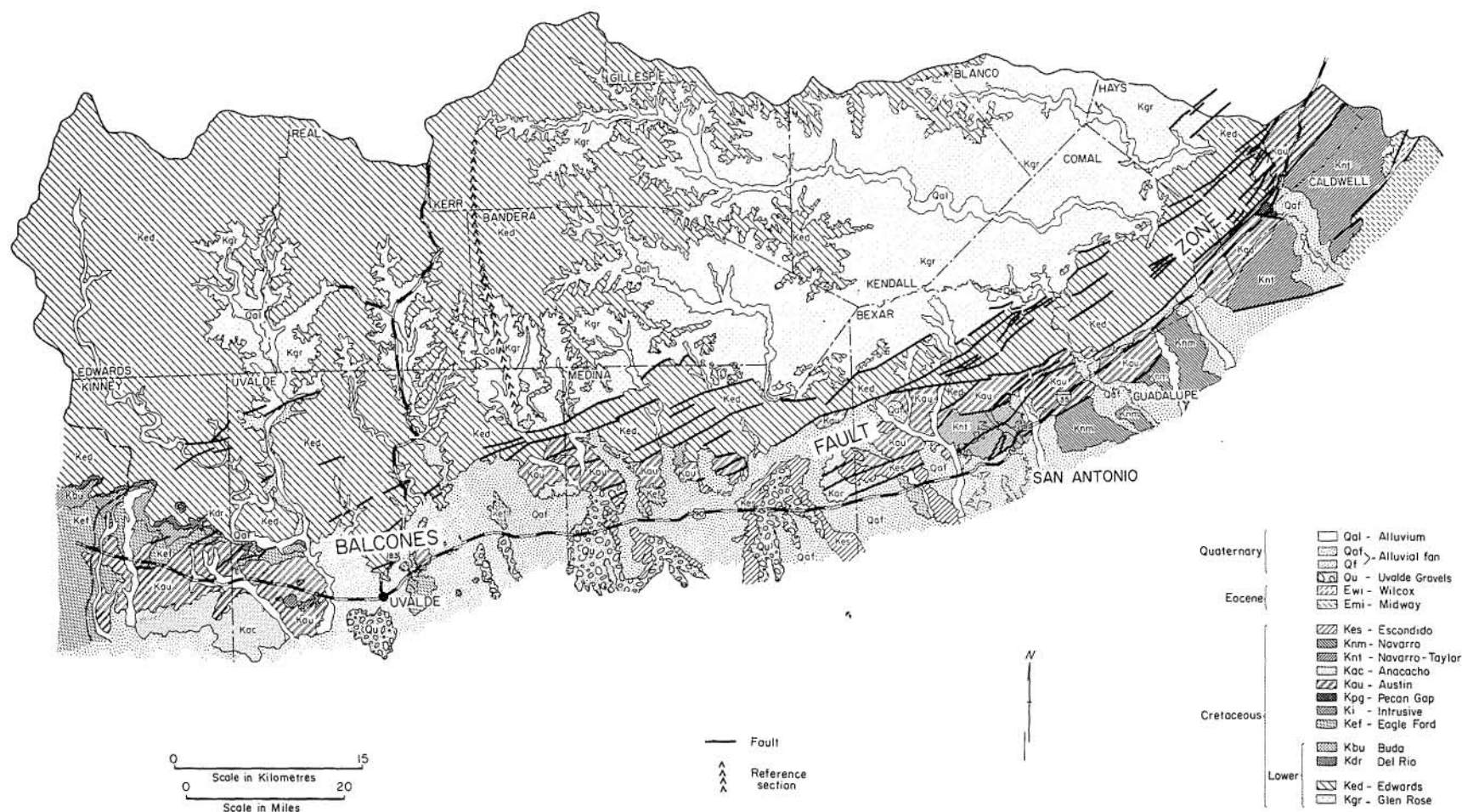


Figure 2. Geologic map of southern Edwards Plateau.

which clay beds rarely occur. Although the marly limestones of both the Glen Rose and the Edwards formations are rapidly weathered and eroded, they contain only a minor component of clay minerals. In general, Glen Rose outcrops appear less brittle and may have fewer through-going fractures than the Edwards lithologies.

The southern limit of both the Glen Rose and Edwards outcrops occurs along the Balcones fault zone which strikes east in the western part of the study area (fig. 2) and nearly northeast in the eastern part. North of the major faults, broad valleys expose wider outcrops of the Glen Rose Formation. Valleys of alluvial deposits become narrow immediately south of the northern limits of faulting as streams incise the downdropped Edwards Limestone. Displacement along the Balcones fault zone is a maximum of 520 m in the east (DeCook, 1963), and 215 m in the southwest (Welder and Reeves, 1962). Maximum displacement is about 150 m along eastern faults and about 60 m along western faults. The Balcones fault zone is a major region of recharge, especially where it is transected by streams in flood.

The terrain flattens over the producing zone south of the Balcones fault zone and its terminal escarpment. Two major lithologic units crop out at that point: (1) a Cretaceous succession of slightly calcareous mudstones and chalks (Eagle Ford, Austin, Taylor, and Navarro); and (2) broad, extensive Quaternary gravels and sands in the form of fanplains beginning just down dip of Balcones faulting. The clasts in these fan sediments are nearly all carbonate, but sparse chert does occur. The fan sediments are subaquifers which are recharged on their surface; however, it is doubtful that they recharge the Edwards aquifer down faults which generally transect thick mudstones.

A simplified version of the general hydrogeology of the Edwards aquifer follows. In the north, recharge is predominantly into vertically fractured Edwards limestones and dolomites, and the Edwards Limestone is itself an unconfined ground-water system. Water migrates southward, discharging at various locations from surficial springs at the base of incised Edwards outcrops. Where the harder Glen Rose limestones and dolomites are well fractured, they are infiltrated by vertically moving fluids, but the softer limestones are usually permeability barriers. Water also infiltrates into and migrates southward in the alluvial systems with some vertical fractures. Maximum vertical recharge occurs in the Balcones fault

zone, especially during flooding (Green, 1967). South of the fault zone there is major water storage at shallow depths in downfaulted Edwards limestones; minor volumes of water are stored in thick, lower Glen Rose limestones which are rarely connected vertically by fractures to overlying Edwards carbonates.

METHODOLOGY FOR MAPPING FRACTURE ZONES

In order to map fracture zones in a large region, a method of computerizing the interpretations of aerial photographs was developed to take advantage of data processing and reduction. Field measurements of joints were not selected as the primary data-gathering method because gaining access to privately owned land, as well as actually measuring joints, both take considerable time. It has been previously demonstrated that faults and fracture zones are mappable on aerial photographs as lineations (Wermund, 1955; Lattman and Nickelsen, 1958), and that such fracture zones relate to ground-water production in carbonate terranes (Lattman and Parizek, 1964).

Fracture Trace Mapping

Lineations, or fracture zones, are features of variable contrast where identified on aerial photographs (fig. 3). Various kinds of known lineations include straight stream segments, darker toned linear traces in unvegetated soil or rock with greater moisture content, and relatively straight vegetation alignments. To be certain that the orientations of fracture zones (lineations) were not distorted, the fracture traces were identified on controlled mosaics of 1:24,000 black-and-white aerial photographs by Tobin Aerial Surveys. These mosaics are identical in size and scale to the standard U.S. Geological Survey 7.5-minute topographic map.

Two kinds of fracture traces were identified: short and long sets. Short lineations (up to 4.5 km) were identified on photographs in reflected light, and the interpreter generally studied the photomosaics singly at different viewing heights. The end point of each lineation was identified with an arrow. Each photomosaic or quadrangle was examined by three interpreters, each of whom spent about 20 minutes viewing a specific photo. (An exception was a strip of 12 quadrangles which are identified below.) Cepeda

(1974) determined that the data are biased depending on the viewing time: a longer viewing time, in either one or multiple viewing sessions, results in the identification of more lineations.

The long fractures are up to 160 km in length. Before identifying long fractures, researchers taped all the mosaics for the area on a ballroom floor. Next, they sighted across the mosaics in reflected light, in this way locating each long, apparent lineation. No long fracture was accepted unless three or more geologists agreed on its position. On reaching such agreement, the geologists marked the lineation with tape for later transfer in ink onto the back of the mosaics.

Digitization

Following identification, researchers traced the lineations representing long fractures as lines on overlying paper and marked the quadrangle corners. Each quadrangle (photomosaic) was given a 6-digit identification number based on arbitrary x,y coordinates. These coordinates were used in a digitization program with a 0,0 point at the southwest corner of each quadrangle. The coordinates (x_1,y_1 , and x_2,y_2) for each end point of the short fractures were read mechanically within each quadrangle. Readings were registered to the nearest 0.25 cm. Initially, all coordinates with quadrangle identification were punched onto cards; later, all information was read onto magnetic tape.

In a similar manner the long fractures were punched onto a separate subset of cards. Each long fracture was identified by a successive number chosen arbitrarily. Coordinates were identified by quadrangle plus the x,y coordinate of an end point within a quadrangle.

Although each fracture zone was physically marked as it was digitized, verification seemed essential; therefore, a drawing of the fractures was reproduced to check against the input sheets. Errors were rare—less than 0.5 percent.

Computation

It became evident early in the study that digitization and computer calculations would be essential. There are 177 quadrangles, each averaging about 400 short fractures. Each short fracture had to be identified as two end points (x_1,y_1 , and x_2,y_2). Fracture zone identification required nearly 300,000 signatures with three or more integers. In addition, the length and azimuth were both necessary

calculations and storage elements. Finally, another subset of integers was necessary to identify the end points of the long fractures. Computer programs were designed to display the detailed distribution of the short-fracture calculations on a variety of maps (Wermund and others, 1974a). Moving averages of the density and orientation of fractures were computed for maps as (1) number of fractures, (2) length of fractures, and (3) number of fracture intersections. All averages were computed per unit area.

The size of the unit area (floating grid) and the amount of overlap could both be arbitrarily selected to relocate the floating grid, providing the moving average. These were two of the options in new programs written first to determine and then to display values reflecting incidence, length, intersections, and orientation of fracture zones. A contour package owned by the Texas Water Development Board was used for selected displays of results. A further option in the program was the selection of an area to be mapped; the largest area was limited arbitrarily to 36 quadrangles. A single display of the entire study region (fig. 4) was assembled by overlapping eight of the largest possible areas. Programs (see appendix) display fracture density data on contoured maps; fracture orientations are graphic displays.

For this study the regional orientations of the short fractures are displayed as a rose diagram for each individual quadrangle. These rose diagrams display 10° classes, but programming allows plotting of other classes as well. The number of short fractures is also calculated and plotted for each quadrangle. A hand-contoured map of the regional-fracture incidence is shown by number of fractures per 7.5-minute quadrangle. (A quadrangle encloses slightly less than 170 km^2 at the latitude of the study area.)

Only one program permits plotting at any scale of the long fractures, and in this regional study that plot is used to relate long-fracture zones and geology.

Field Test

Although other investigators have stated that aerial photographic measures of fracture zones show agreement with field measurements of joints, the writers believed that this investigation required a specific field test. A test area of 36 quadrangles was selected for examination (fig. 1). This same test area was also used for program debugging and bias analysis.

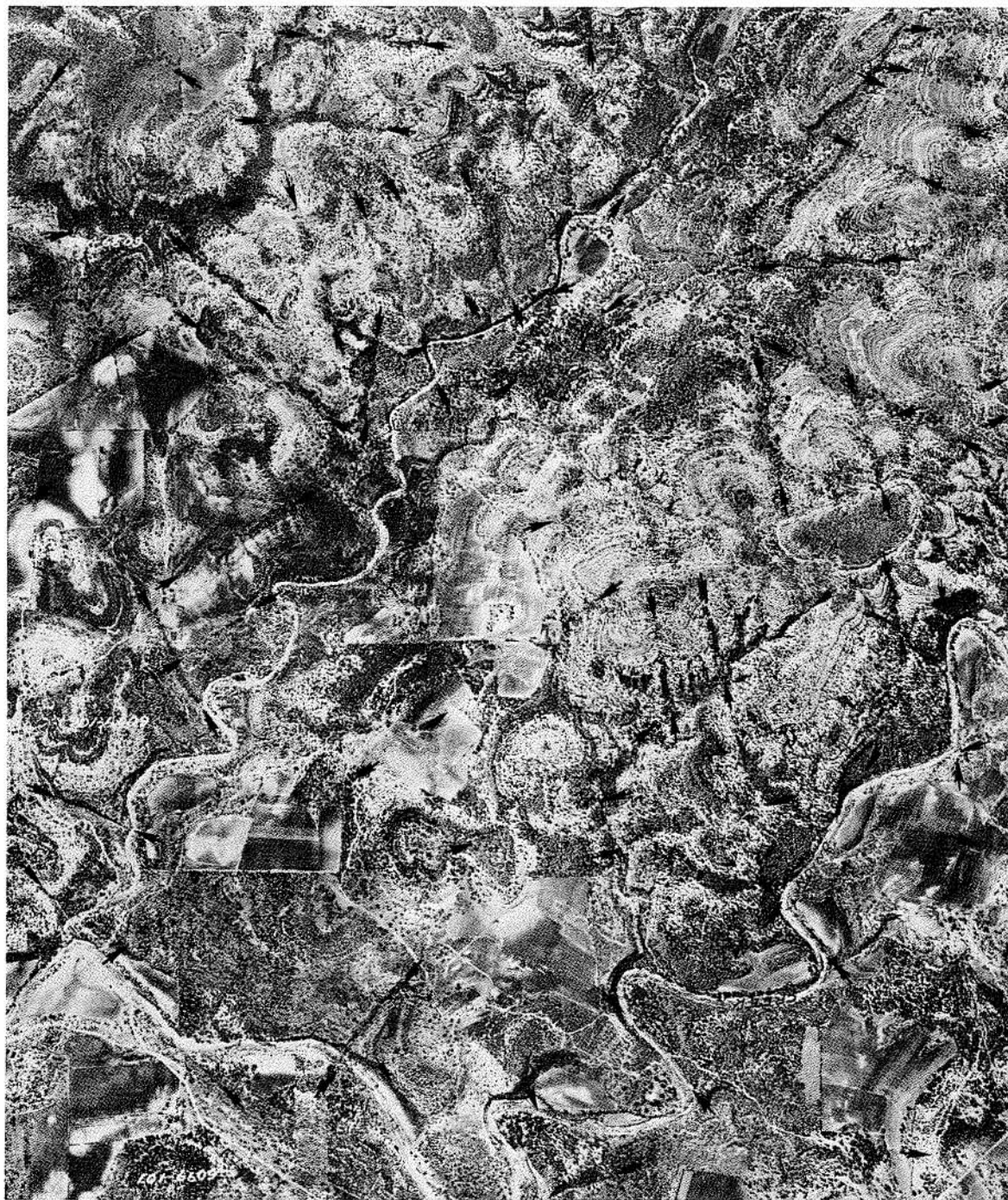


Figure 3. A part of a controlled mosaic of black-and-white aerial photography on which arrows indicate the limits of fracture zones.

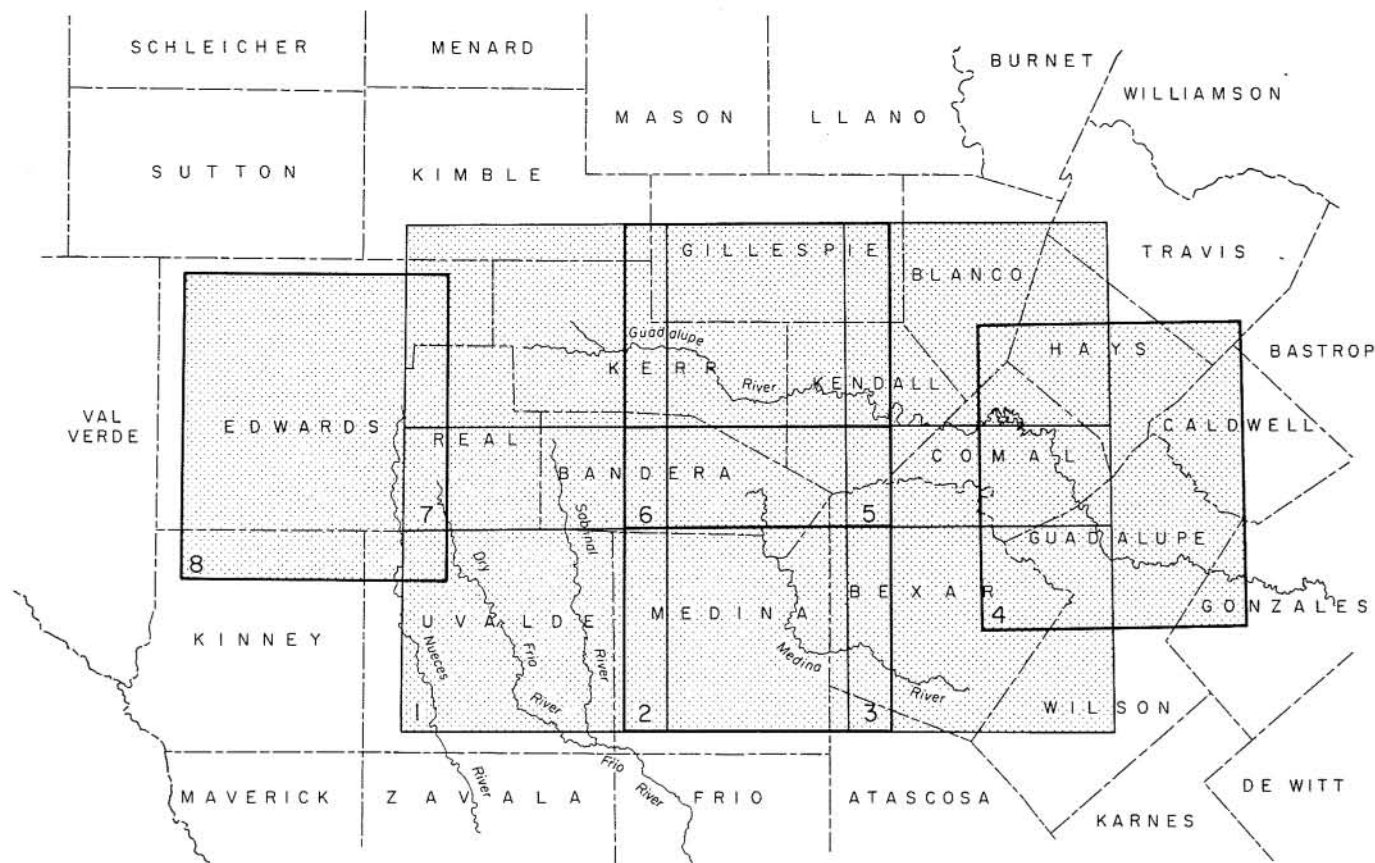


Figure 4. Areas of 36 quadrangles, each of which was composited for regional fracture analysis.

The test site included the area of maximum dissection in the southern Edwards Plateau, with most land area in valley walls. Relief approximated 358 to 500 m in the dissected plateau and 115 m in the coastal plain. The geology of the test area is representative of the entire regional geology (fig. 2); only the widespread plains of calcareous muds are absent in the southern part of the test area.

In the test area joints were measured at 320 stations (fig. 5), primarily along roads. Most joints were measured as through-going fractures in hard limestones and dolomites. Another group of joints was frequently observed and measured in outcrops of the soft marly limestones which are easily eroded, forming recessive topography in the Glen Rose Formation. In the valleys, joints were also measured in indurated alluvial deposits, including terraces and alluvial fans. The lithology of these latter deposits is usually gravel cemented by caliche; caliche deposits thicker than

0.25 m are commonly well jointed, even on the divides. Wherever possible, all types of joints were measured on a broad flat outcrop with an unobstructed vertical view.

Joints were subdivided arbitrarily into three types. On a horizontal exposure, type I joints were observed as abundant, parallel, through-going fractures generally open at the top. They usually control development of both soil and vegetation as a result of increased weathering on joint surfaces. In vertical outcrops, type I joints always transect the entire outcrop, are abundantly represented, and are commonly infilled by some soil. On a horizontal exposure, type II joints were exposed parallel fractures, usually tight and rarely supporting vegetation. In vertical outcrops, type II joints generally cut the entire crop but never fill with soil. Type III joints are sparse, tight, and commonly isolated in a few beds in all attitudes of exposure. Veins and fracture fillings

were included as type III joints if they entirely transected a limestone bed.

Following joint mapping, rose diagrams were manually constructed for each quadrangle. In representing the orientation of both joints (fig. 6) and fracture zones (fig. 7), the size of each rose diagram was proportionate to the incidence of fractures for each 7.5-minute quadrangle. In any one rose diagram, the length of each class, 10° to 20° , for example, was proportionate to the representation of that class; the same arbitrary increment equaled one measurement in all the displays of orientation for one phenomenon. Because the type I joints were most visible and type III joints were least visible on aerial photographs, the joint measurements were weighted according to type in summing the classes. Type I joints counted three; type II counted two; and type III counted one.

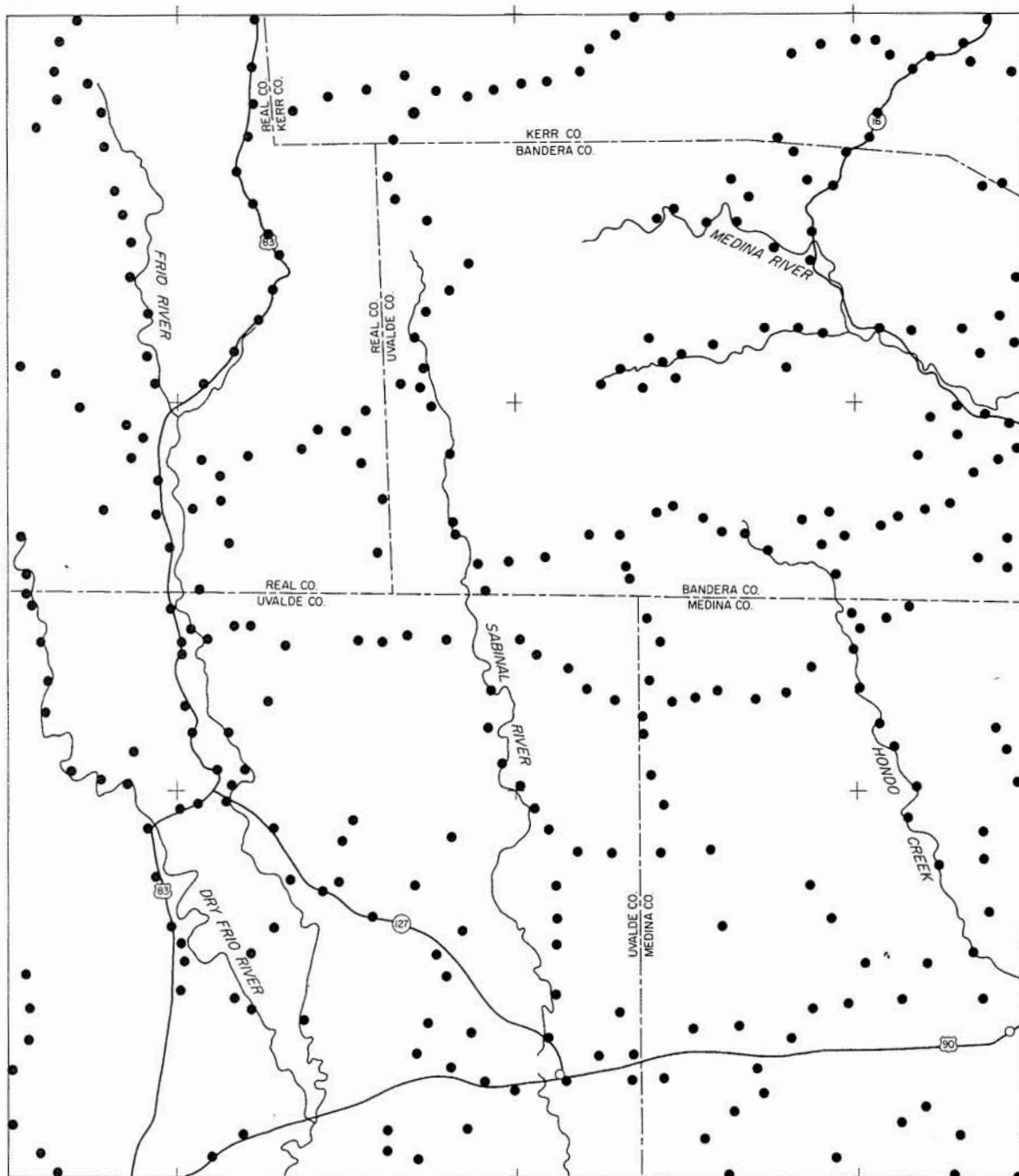


Figure 5. Locations where field measurements of joints were determined in the test area; measurements emphasize orientation over incidence.

Finally, a visual comparison of the strength and orientation of the same classes was made for joint-rose diagrams and fracture-zone diagrams. Substantial general agreement existed between the orientations measured in the field and those measured from aerial photographs. The largest observable variation was that field measurements indicated stronger and more abundant north-south and east-west fractures than did aerial photographic measurements. This variation may be a result of the fact that in using aerial photographs, an observer may have difficulty separating natural features from man-made features, such as fences or trails, which commonly trend north-south and east-west.

Caves

The results of mapping caves in the southern Edwards Plateau were collected by Luttrell (1975) either from published papers or from files of the Texas Speleological Society (courtesy of Ron Fiesler). Two geometric shapes of caves occur as end members. In linear caves, caverns interconnect with long linear passages (fig. 8). The oblate caves occur with almost oval or elliptical chambers connected to linear passageways, or they are isolated as single large caverns. Although the latter geometry distorts the data slightly, rose diagrams were plotted at the location of each cave type. The rose diagrams for caves were constructed differently from the rose diagrams for joints and fracture zones. For caves, all rose diagrams are the same size regardless of the number of measurements; the length of the bar representing each class shows the frequency of fracturing as a percent.

REGIONAL DISTRIBUTION OF FRACTURE ZONES AND CAVES

Short-Fracture Orientation

Despite the varying sizes of the roses, inspection of the regional orientation of short-fracture zones (fig. 9) shows that northwest and northeast directions are generally equally represented in most roses (135). Where the roses are skewed, the roses with a dominant northwest limb (29) are more common than those with a larger northeast limb (13). It is also obvious that the most abundant fracture sets strike approximately $N 40-60^{\circ}W$ and $N 40-60^{\circ}E$. The next

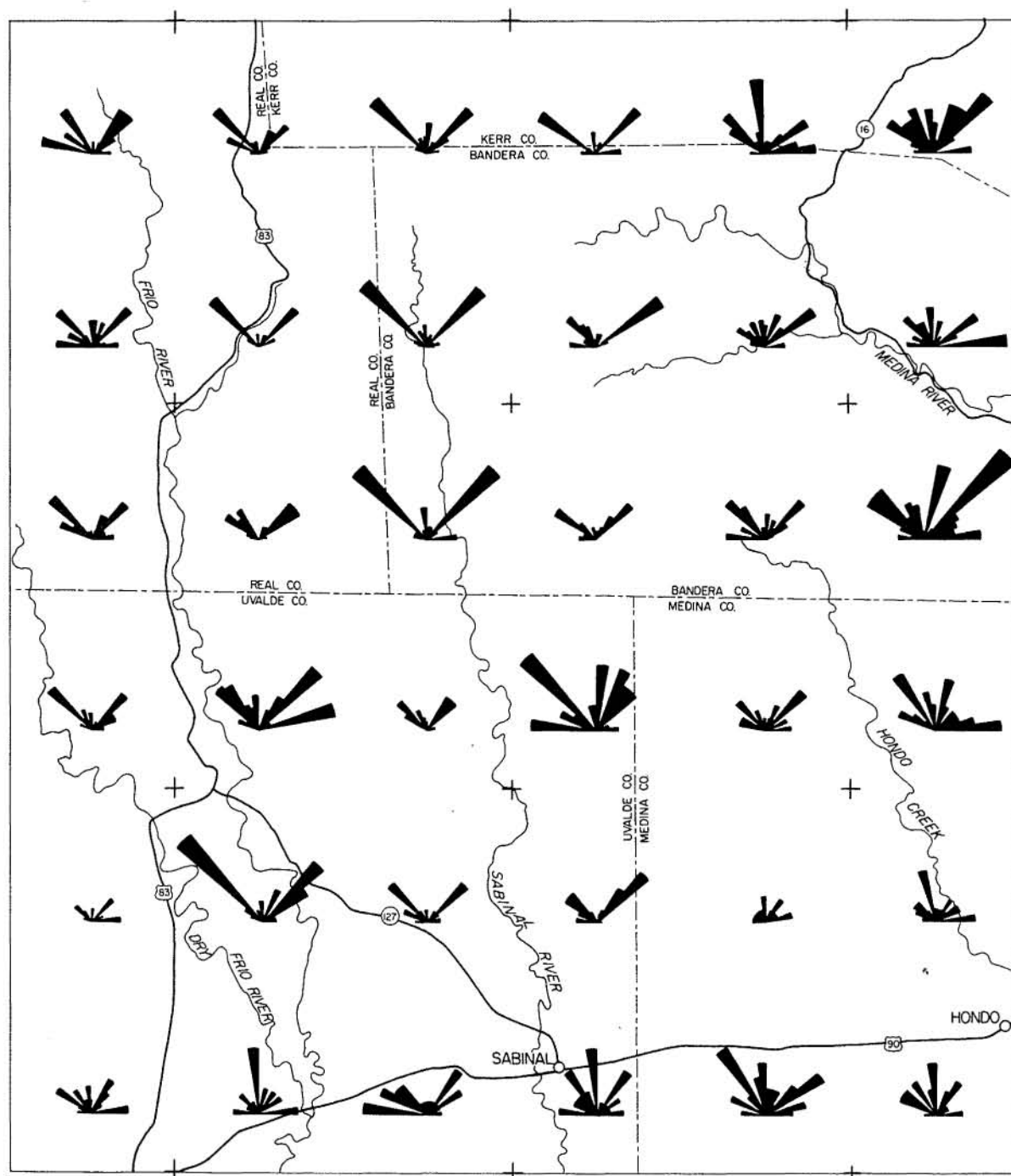


Figure 6. Orientation of joints in the test area displayed as rose diagrams with 10° classes; each rose sums measurements in a 7.5-minute quadrangle. Length is proportionate to significance of occurrence as described in text.

most common fracture set strikes east-west; north-south sets are less common. Complementary sets trending near $N 20^\circ W$ or $N 20^\circ E$ are rare; if present, only one of the sets generally dominates.

In the western quarter of the map in the Nueces River drainage basin, east-west sets heavily influence the rose pattern. For the remainder of the drainage area in the southern Edwards Plateau, the $N 45^\circ W$ and $N 45^\circ E$ sets are balanced. In the eastern and south-eastern peripheries of the study area, fracture sets trending from $N 20^\circ W$ to $N 20^\circ E$ are prominent.

Comparing the distribution of rose diagrams (fig. 9) with the geologic map (fig. 2) reveals no strong correlation. Outcrop patterns and stratigraphic variations do not influence the orientation of short fractures. Most surprising is the apparently weak coincidence of short-fracture roses with the principal faults of the Balcones fault zone.

Short-Fracture Incidence

The regional incidence for the number of short fractures per quadrangle varies from 101 to 718 (fig. 10). The average incidence is 368 short fractures per quadrangle. The lowest fracture incidence occurs in the southeastern part of the study region, the area south and east of the Balcones fault zone. This area is dominated by outcrops of extensive alluvial plains—Qaf and Qf—and of mudstones—Kaf, Knt, and Knm (fig. 2). These stratigraphic units are generally cultivated, masking the recognition of fracture zones and representing a clear bias recognized early in developing the method (Cepeda, 1974). On a detailed fracture-incidence map constructed from aerial photographic identification of fractures, very low fracture abundance correlates closely with a land use map identifying cultivated fields.

Fracture-zone abundance is not consistently large in the Balcones fault zone (fig. 10). There is also no regular increase or decrease in the number of fractures at a distance from the major faulting. In the area of the dissected Edwards Plateau, fracture zones are no more prominent in Edwards Limestone than in the Glen Rose Formation (fig. 2). Therefore, fractures in the recharge zone do not appear to be controlled by rock type.

One area of apparent higher incidence occurs on the orientation map for short-fracture zones (fig. 9) as a series of 12 roses immediately north of Uvalde, and on the map of fracture incidence as a high located over the valleys of the Dry Frio and Frio Rivers. This area was originally a test strip of

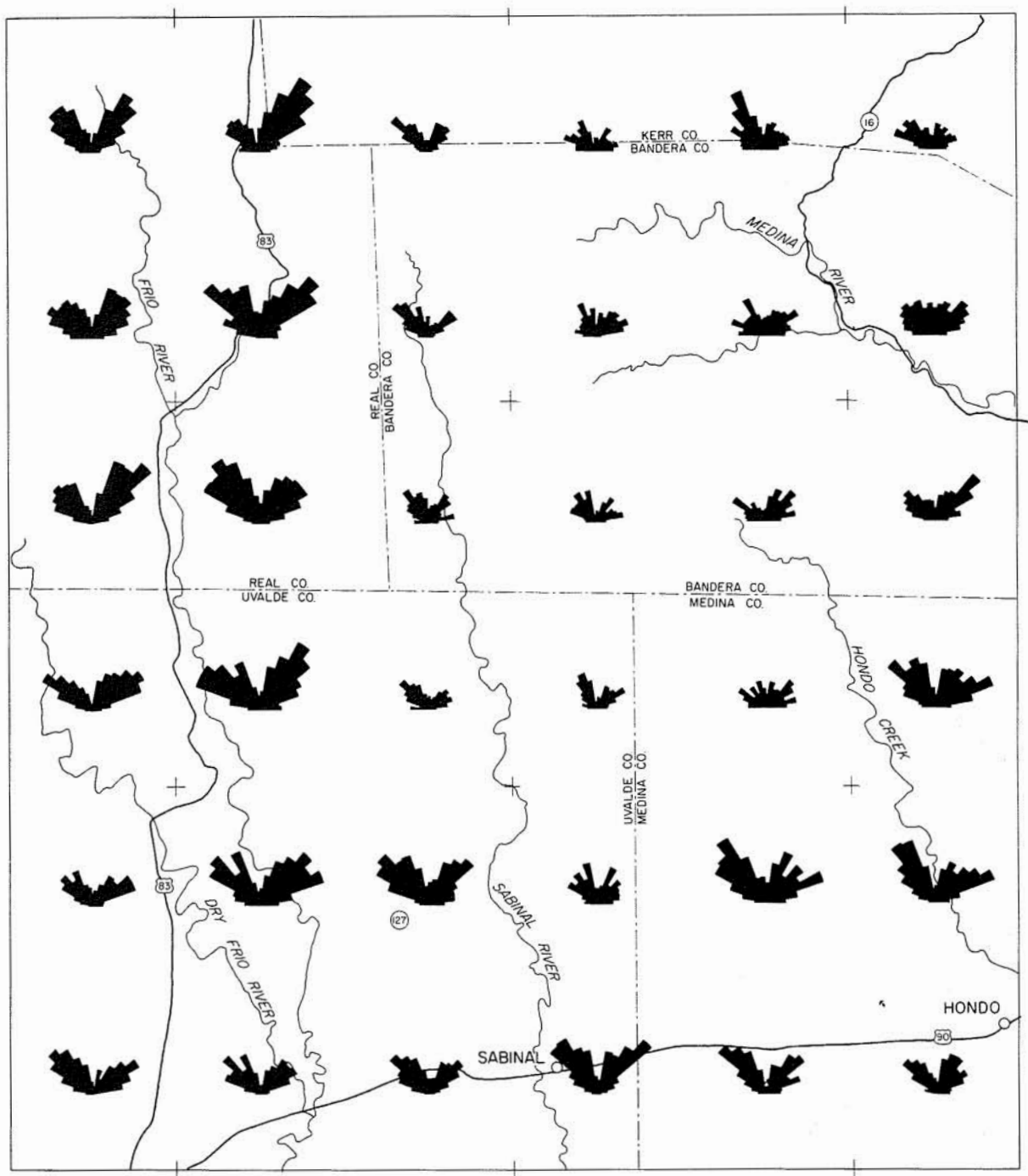


Figure 7. Orientation of fracture zones in the test area displayed as rose diagrams with 10° classes derived from interpretation of lineations on controlled mosaics of black-and-white aerial photography.

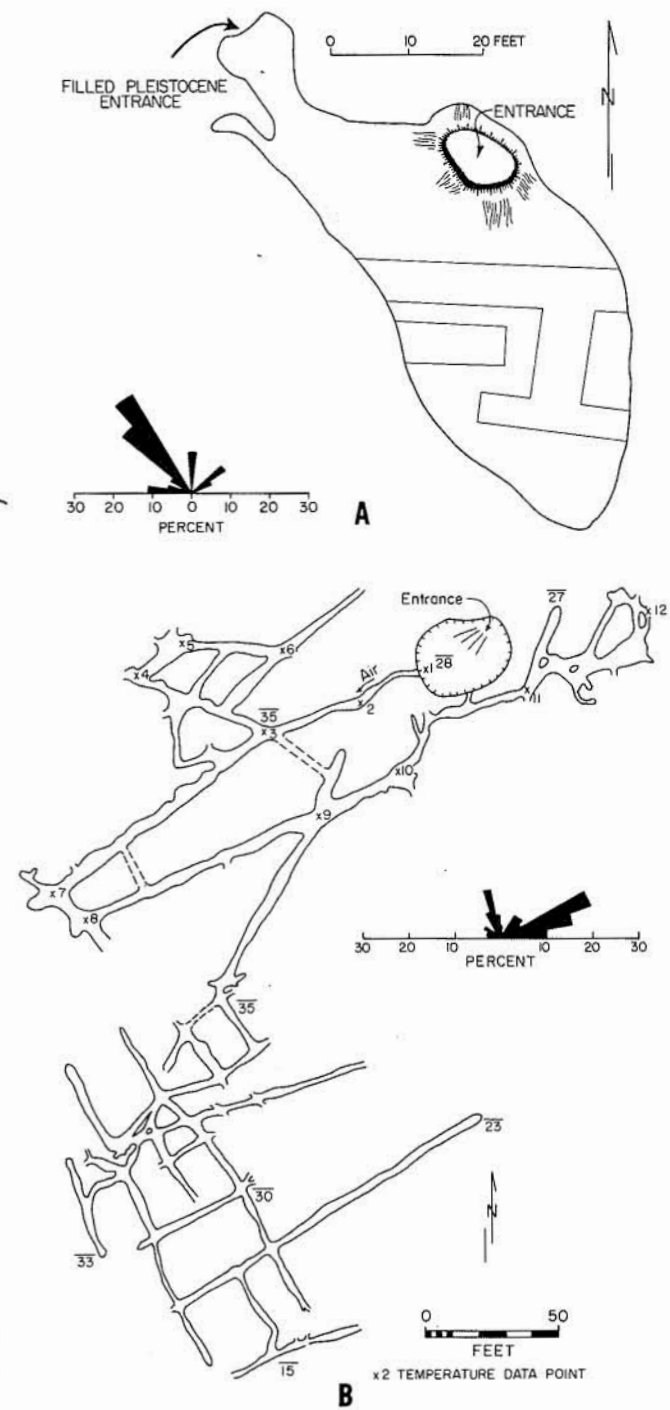


Figure 8. End members of variable cave geometry shown as (A) oblate caves, and (B) linear caves; rose diagrams illustrate interpretation of respective orientations.

12 quadrangles used to derive a method of environmental geologic mapping in carbonate terranes (Wermund and others, 1974b). More time was spent identifying short fractures on the 12 mosaics of this small test strip than on fracture incidence in any other locale. It was here that Cepeda (1974) identified one methodological bias: more time studying photographs yields more identified fractures. An adjustment has therefore been programmed into the displays of orientation and incidence by proportionately decreasing the size of roses and the incidence of these 12 quadrangles relative to the block of 36 originally plotted quadrangles. Even after this statistical adjustment, however, some bias remains.

Long Fractures

As might be expected, the orientation of the long fractures (fig. 11) is similar to that of the short fractures. Northwest- and northeast-trending sets are most prominent. In the vicinity of the Balcones fault zone, many long lineations represent single faults or zones of faults. Except in the west, few north-south

and east-west long fractures are evident. Most north-south- and east-west-trending long fractures occur north of the fault zone.

A negative bias exists in interpreting the north-south and east-west fracture zones—an interpreter hesitates to report these orientations because cultural features and property boundaries in the United States are generally oriented north-south or east-west. This orientation is common even in Texas, with its irregular land system. A further complication results from the use of controlled aerial photomosaics. Numerous mosaic tears orient north-south and east-west. Therefore, the authors suspect that more north-south and east-west fractures occur than are shown in this work. This conclusion is supported by the incidence of readily measured joints with north-south and east-west orientations (fig. 6).

There are a large number of long fractures in the western quarter of the plateau. The incidence is also great in the eastern half of the region but not especially so in the Balcones fault zone. Large and short fracture zones generally coincide in the eastern

half of the study region.

Caves

Most mapped caves (fig. 12) are located in the Edwards Limestone (fig. 2). A few caves exist in lower Glen Rose limestone, but they are not common. Overlaying a cave map with the geology map shows that oblate and linear caves are equally represented in the Edwards Limestone, whereas oblate caves are more abundant in the Glen Rose Formation.

There are a large number of caves in the Edwards Limestone where the formation crops out on the divide between the Nueces and Rio Grande Rivers. This region includes the area described above as having most of its land in the divides. Along the northern border of the study region, only a few Edwards caves occur where a divide separates drainages of the study region from the Colorado River. A distinctive southern belt of caves is located entirely in down-faulted Edwards carbonates of the Balcones fault zone.

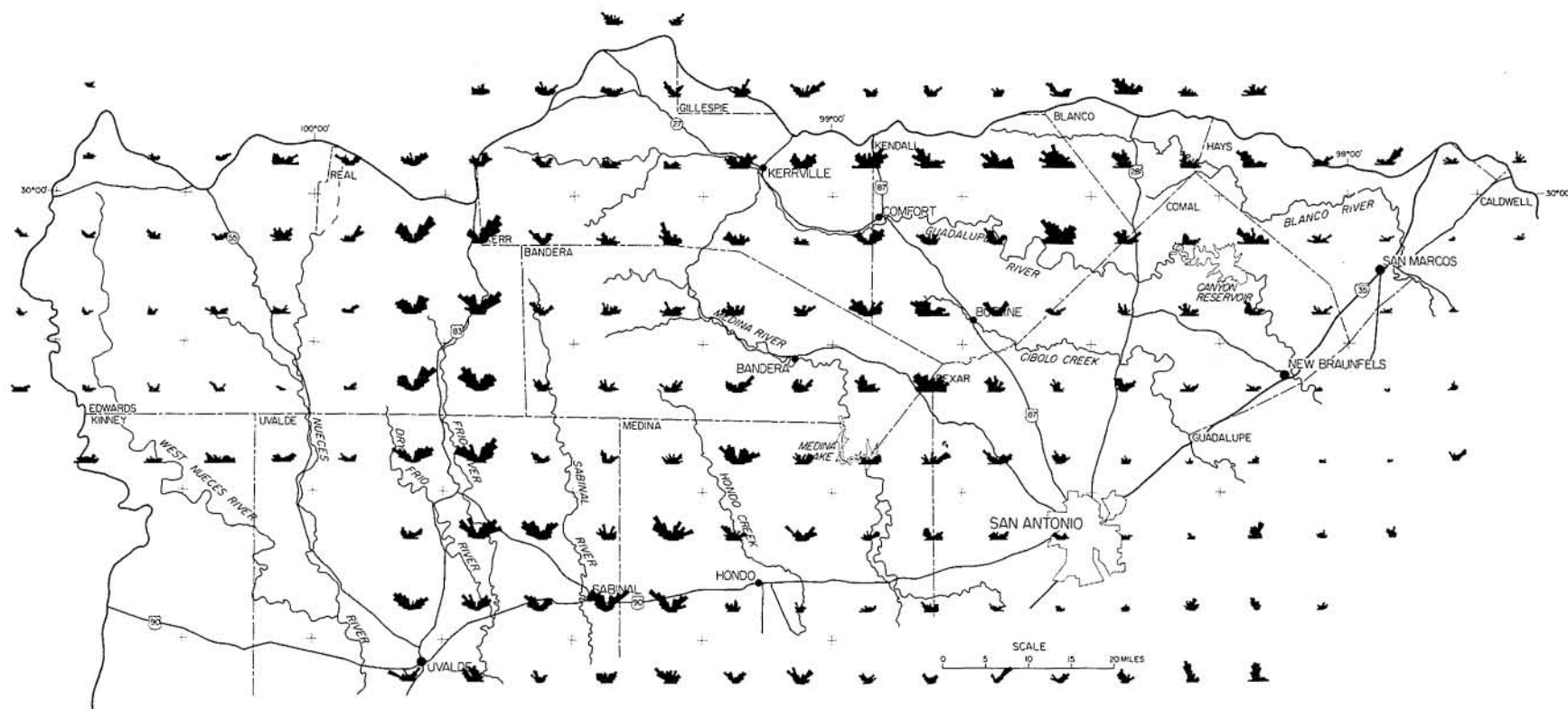


Figure 9. Orientation of short-fracture zones.

An obvious correlation exists between caves and normal faults of the Balcones fault zone. That correlation is most evident in the eastern half of the southern Edwards Plateau, where cave passages between N 80°E and N 50°E are abundant. Cave limbs commonly orient east-west and north-south in this region and may be related to shear fracture sets. Other common classes described in the orientation of short fractures occur less frequently.

West and north of the main zone of Balcones faults, northwest and northeast limbs are abundant in the caves, and north-south limbs are common. In all areas cave roses have more clearly defined and separated classes than do roses of short fractures.

Comparing the incidence of caves (fig. 12) with the incidence of short fractures (fig. 10) shows that cave frequency increases as fracture incidence increases. This coincidence is surprising in areas the size of a 7.5-minute quadrangle. A visual comparison of the same two maps, however, shows no apparent

prevalence between cave type and fracture incidence.

In overlaying maps of caves and long fractures (fig. 11), the authors found no apparent relationship between the frequency of occurrence of caves and of long fractures. As with short-fracture orientation, a moderate coincidence of the orientation of caves with the orientation of long fractures was observed, especially in the Balcones fault zone.

METHODOLOGICAL BIAS

Having summarized the observations of fracture orientation and incidence, the authors will summarize those biases which influenced their interpretation of these factors before discussing their meaning. Cepeda (1974) studied the test area used in this project to compare field and laboratory measurements (figs. 5-7). He compared the inherent properties of the aerial photographic mosaic, the viewing time involved, and computed maps of fracture zones. He

also compared the maps with topography, lithology, vegetation, and land use. To correlate this information with local topography, Cepeda used detailed fracture-incidence maps which were overlain by slope maps with units of less than 5 percent, 5-15 percent, 15-25 percent, and greater than 25 percent. He found no apparent correlation. He also compared fracture-incidence maps with maps of lithology, vegetation, and land use. Only land use influenced the identification of fracture zones because fracture incidence decreased over cultivated croplands. Plowing exerted a clear bias on systematic fracture interpretation.

Next, the results of fracture-zone mapping were examined for any inherent bias resulting from our method of interpreting fracture zones. Three biases were apparent. One is the effect of viewing time: longer examination yields more fractures. Second is an edge effect: fractures are more readily identified in a large viewing field. In an initial printout of the detailed incidence of fracture zones, a marked

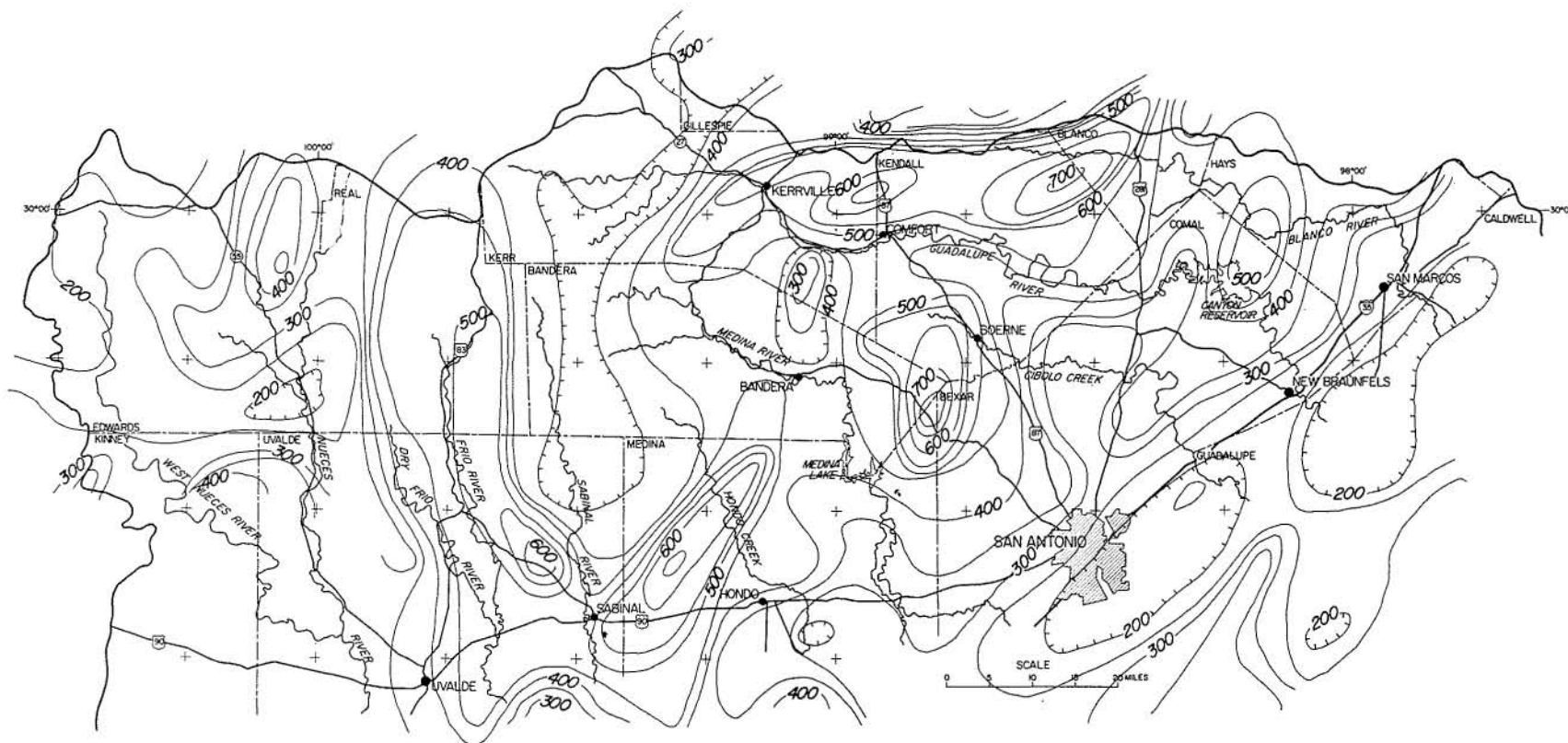


Figure 10. Incidence of short-fracture zones.

fault zone. Indeed, the strongest fractures orient northwest and northeast, with secondary trends north-south and east-west. Probably the north-south and east-west fracture zones occur more frequently than they are mapped because of the mapping bias discussed above. The authors suggest that these independent fractures belong to an older system. In the nearest exposures of basement rocks, about 90 km north to the Central Mineral Region of Texas, high-angle faults, probably Paleozoic in age, trend northeast and north-south and form lines of Precambrian metamorphic rocks which trend northwest (Bayley and Muehlberger, 1968). These trends agree with predominant trends of long and short fractures in the region of the Edwards Limestone aquifer (fig. 13).

Fracture abundance is also measured over

younger structures like the Balcones fault zone. If the long- and short-fracture zones were strongly controlled by Balcones fault events, a higher incidence of fractures in the Balcones fault zone could be expected, with a regular decrease of incidence northward. No such regular pattern was observed.

Caves

Caves are obviously controlled by the long- and short-fracture systems mapped in this study (figs. 9-12). It may be that long fractures are more important in cave formation than are short fractures; the evidence at this time must be considered weak. In the Balcones fault zone where long fractures parallel the principal faults, certain cave limbs also strongly parallel faulting (fig. 12). Beyond the limits of

Balcones faulting, the caves parallel both long and short fractures of the older basement structures.

Two concentrations of caves can be clearly differentiated. One group occurs in the eastern part of the study region, including the most recently dissected Edwards Plateau of the Balcones fault zone; the other appears in the western and northern study region containing the oldest surface and least dissected Edwards Plateau. In the latter area, most of the surficial land lies in broad divides between drainage. These circumstances appear to lend support to a theory of two separate ages of cave formation. Additional evidence seems to exist in our observation that for two mapped caves the basement system of fractures is more prominent in the west, and the Balcones system of fracture zones is more conspicuous in the east.

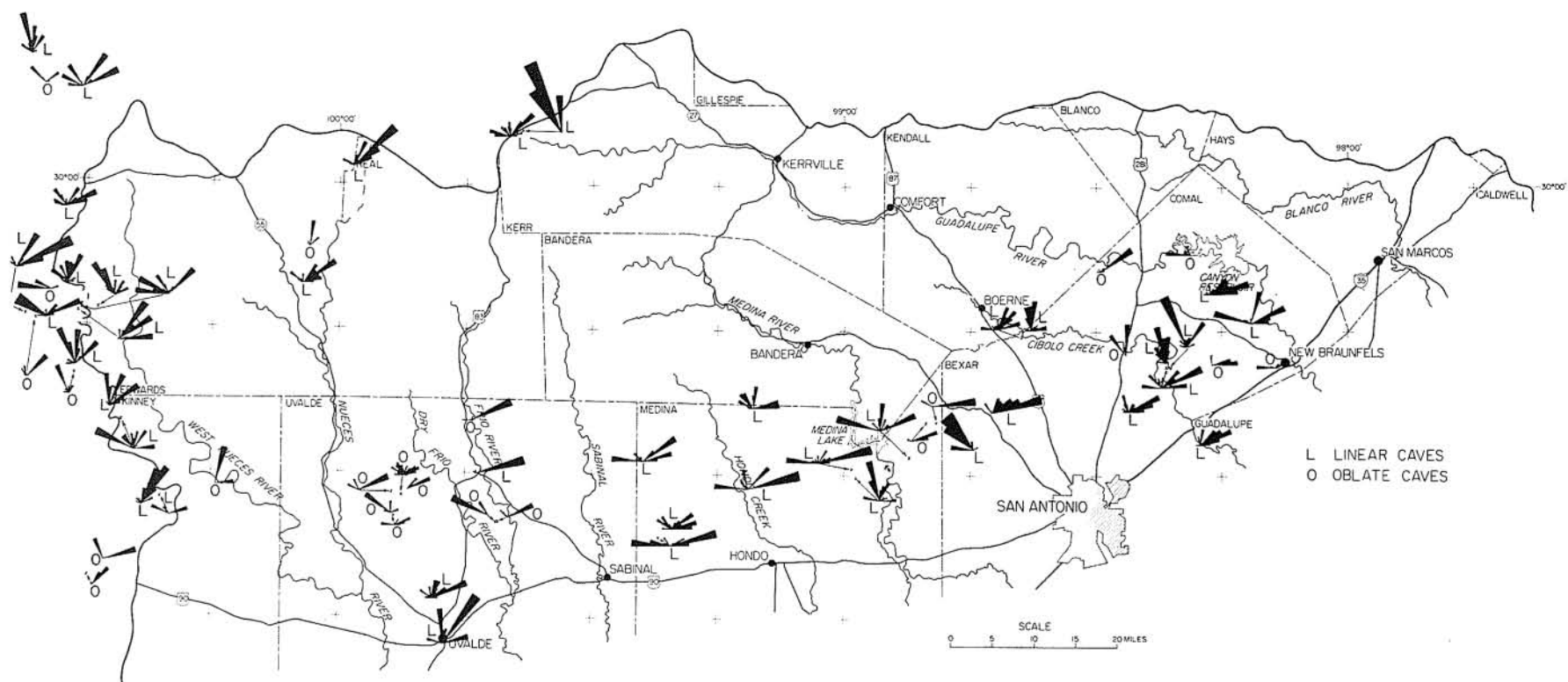


Figure 12. Distribution and orientation of caves.

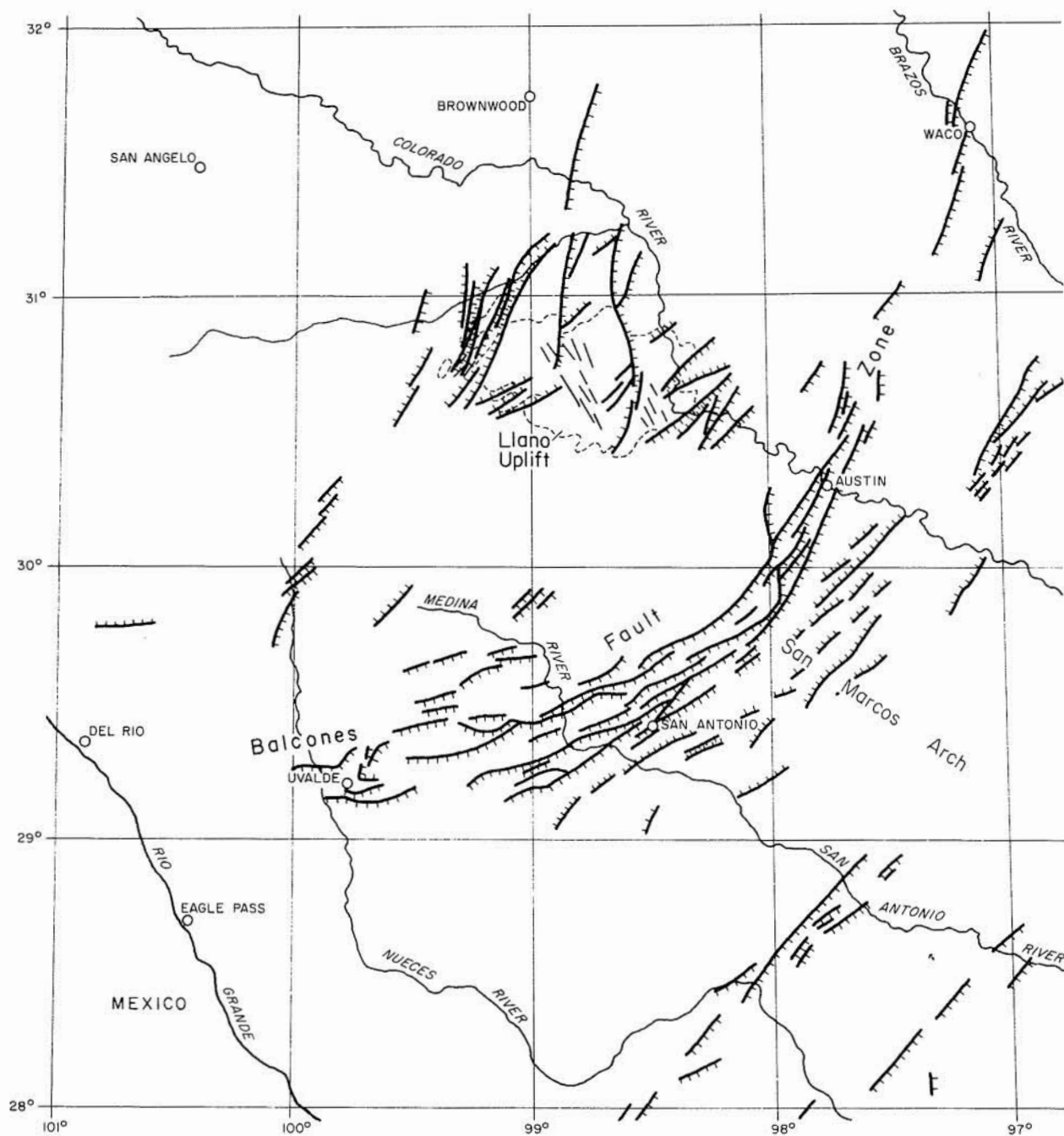


Figure 13. Tectonic elements surrounding the southern Edwards Plateau (after Cohee, 1962, and Bayley and Muehlberger, 1968.) The Llano uplift is an area of exposed Precambrian basement in which the northwest-trending elements parallel schistosity and gneissic banding, whereas northward- and eastward-trending structures are normal faults.

MAJOR CONCLUSIONS

1. A method combining aerial photographic interpretation, digitization, and computer analysis may be an important aid in developing rapid regional mapping systems of the fracture zones. Such maps yield an understanding of the vertical porosity/permeability in the zones of recharge and production for large carbonate aquifers.
2. In the region of the Edwards Limestone aquifer of South Texas, the dominant northwest and northeast, and secondary north-south and east-west orientations of fracture zones are not controlled by the Balcones fault system. A fracture system related to older structural events probably influenced these trends.
3. Within the Balcones fault system, the principal faults and related fracture zones strongly affect the eastward- and northeastward-trending passages of caves. Away from Balcones faulting, caves orient strongly northwestward and northward, parallel to fractures of older tectonic events.

ACKNOWLEDGMENTS

Major support for this research was provided by a contract with the Texas Water Development Board, IAC (74-75)-1207. In addition, David Ferguson, T.R. Evans, and Charles Tucker of that agency's Computer Center Division contributed technical assistance including digitization, computation, and plotting of initial results. Seth Burnitt, Texas Water Development Board, was the contract manager and a constructive critic of this study.

In the Bureau of Economic Geology, valuable contributions were made in fracture zone identification by research assistants including Ann Bell, Judy Ann Russell, and David Walz. Assistance in designing preliminary algorithms and programs for computation was contributed by Ann Bell; final production of computer printouts of fracture data in 1975 was supervised by Ray Leonard.

Review of a preliminary manuscript was thoughtfully provided by William R. Muehlberger, Department of Geological Sciences, and by Charles W. Kreitler and Robert A. Morton, Bureau of Economic Geology, The University of Texas at Austin. The authors are grateful to all those who so willingly contributed their time and professional concern.

REFERENCES

- Barnes, V.E., project director, 1974a, Austin sheet: Univ. Texas, Austin, Bur. Econ. Geology Geol. Atlas of Texas, scale 1:250,000.
- _____ 1977, Del Rio sheet: Univ. Texas, Austin, Bur. Econ. Geology Geol. Atlas of Texas, scale 1:250,000.
- _____ in preparation (a), Llano sheet: Univ. Texas, Austin, Bur. Econ. Geology Geol. Atlas of Texas, scale 1:250,000.
- _____ 1974b, San Antonio sheet: Univ. Texas, Austin, Bur. Econ. Geology Geol. Atlas of Texas, scale 1:250,000.
- _____ 1974c, Seguin sheet: Univ. Texas, Austin, Bur. Econ. Geology Geol. Atlas of Texas, scale 1:250,000.
- _____ in preparation (b), Sonora sheet: Univ. Texas, Austin, Bur. Econ. Geology Geol. Atlas of Texas, scale 1:250,000.
- Coffee, G.V., chm., 1962, Tectonic maps of the United States: Am. Assoc. Petroleum Geologists, and U.S. Geol. Survey, scale 1:2,500,000.
- Bayley, R.W., and Muehlberger, W.R., 1968, Basement map of the United States: U.S. Geol. Survey, scale 1:2,500,000.
- Cepeda, J.C., 1974, Factors influencing fracture data derived from aerial photomosaics (abs.): Texas Jour. Sci. (in press), Texas Acad. Sci., 77th Ann. Meet., p. 10.
- DeCook, K.J., 1963, Geology and ground-water resources of Hays County, Texas: U.S. Geol. Survey, Water-Supply Paper 1612, 72 p.
- Green, M.G., 1967, Artificial recharge to the Edwards Limestone aquifer in south Texas, *in* Hydrology of fractured rocks: Proc. Dubrounik Symposium, October 1965, p. 465-481.
- Lattman, L.H., and Nickelsen, R.P., 1958, Photogeologic fracture-trace mapping in Appalachian Plateau: Am. Assoc. Petroleum Geologists Bull., v. 42, p. 2238-2244.
- _____ and Parizek, R.R., 1964, Relationship between fracture traces and the occurrence of ground water in carbonate rocks: Jour. Hydrology, v. 2, p. 73-91.
- Luttrell, P.E., 1975, Trends in cave passage orientations in southern Edwards plateau (abs.): Texas Jour. Sci., Texas Acad. Sci., 78th Ann. Meet., p. 11.
- Murray, G.E., 1961, Geology of the Atlantic and Gulf Coastal Province of North America: New York, Harper and Brothers, 692 p.
- Rose, Peter R., 1972, Edwards group, surface and subsurface, central Texas: Univ. Texas, Austin, Bur. Econ. Geology, Rept. Inv. 74, 198 p.
- Welder, F.A., and Reeves, R.D., 1962, Geology and ground-water resources of Uvalde County, Texas: Texas Water Comm. Bull. 6212, 252 p.
- Wermund, E.G., 1955, Fault patterns in northwest Louisiana: Am. Assoc. Petroleum Geologists Bull., v. 39, p. 2329-2336.
- _____ Cepeda, J.C., and Bell, A.E., 1974a, Fracture patterns in the southern Edwards plateau, Texas (abs.): Geol. Soc. America Abs. with programs, v. 5, p. 129.
- _____ Morton, R.A., Cannon, P.J., Woodruff, C.M., Jr., and Deal, D.E., 1974b, Test of environmental geologic mapping, southern Edwards plateau, southwest Texas: Geol. Soc. America Bull., v. 85, p. 423-432.
- _____ and Cepeda, Joseph C., 1975, Relation of fracture zones to the Edwards Limestone aquifer, Texas (abs.): Internat. Assoc. Hydrogeologists 12th Internat. Cong. on Karst Hydrology, Abs. and Program, p. 89.

APPENDIX

Computer programs written for this study included

1. SORTFRACTURE
Separates 2 inches of data on edges of quadrangles for later melding together of quadrangles in order to remove edge effects.
2. MERGEFRACTURE
Searches 2-inch strips for matching quadrangles and physically hooks them onto adjacent quadrangles.
3. FRACTURE
 - a. Solves azimuth and calculates 10° classes;
 - b. Searches floating grid of 16 square inches and calculates number of fractures, length of fractures, and number of intersections of fractures;
 - c. Calculates standard deviations of azimuths per 16-square-inch area;
 - d. Calculates weighted arithmetic mean of azimuths per 16 square inches.
4. DUALAZI
Determines and plots lengths of bar representing weighted arithmetic mean in NW and NE quadrants.
5. STADEVI
Determines weighted arithmetic mean and both determines and plots standard deviation envelopes.
6. ROSEDIGM
Takes data from Fracture-Azimuth Subroutine and plots roses.

